JOURNAL OF MATERIALS SCIENCE 29 (1994) 3113–3120

Preparation of YBCO–Ag composites with low carbon contents by a wet method

A. MARIANI, P. L. VILLA*
Dipartimento di Chimica Industriale e Ingegneria Chimica, Politecnico di Milano, 20133, Milano, Italy

$YBa_2Cu_3O_{7-\delta}$/Ag composites were prepared by a wet method, using readily available materials and a modification of the citrate method. This method allows for the addition of silver in soluble form to the YBCO soluble precursor and makes no use of nitrates, thus it allows for a smooth decomposition of the organic substance even in the presence of silver. After decomposition of the organic portion an effort was made to reduce the carbon content by using a gas flow containing N_2 and O_2 with 0.3% nitrogen oxide (NO). The carbon was substantially reduced by operating at high temperature. The pellets obtained from powder so formed were finally annealed at 950 °C in oxygen and then characterized. By increasing the temperature of the NO-anneal a greater spreading of the silver among the YBCO grains was observed. The results show that by this method it is possible to obtain composites in which the only phases detected are $YBa_2Cu_3O_{7-\delta}$ and metallic silver. Although further work needs to be performed on the final products to obtain higher densities and so to obtain improved grain coupling, the data described here open a new way for the production of YBCO-Ag composites with low carbon contents.

1. Introduction

Composite $YBa_2Cu_3O_{7-\delta}$/Ag ceramics are more suitable for practical applications than 1–2–3 materials. The improved properties of composite materials in respect to the 1–2–3 are manifolds. The most important improvement is probably better oxygenation [1–3], this property is ascribed to the easy diffusion of oxygen in silver and it allows a fully oxygenated orthorhombic phase also to be obtained for dense materials with low porosities. Other important improvements are the improved mechanical properties during the annealing steps, due to a reduction in the microcracks formed by anisotropic thermal expansion [4], the improved workability [5] and stability in ambient atmosphere (which are ascribed to the ductility and chemical inertness of silver) and the lower normal-state resistivity [5, 6] which is ascribed to the well-known conduction properties of metallic silver. Silver as a metal has been found to be one of the few metals that does not degrade the superconducting properties of the 1–2–3 [5], while when silver is oxidized to Ag^+ it can partially substitute Cu^{2+} or Cu^{3+} which causes the superconductivity to deteriorate for high levels of substitution [7, 8].

According to the traditional techniques, production of $YBa_2Cu_3O_{7-\delta}$/Ag composites involves mechanical mixing of Ag or Ag_2O with 1–2–3 or 1–2–3 precursor powders followed by several cycles of grinding and calcination at 900–950 °C [4, 5, 9]. These methods cannot provide a good interspersion between silver and 1–2–3 [10]. To overcome this drawback, methods which start from a solution of Y, Ba and Cu cations and Ag are certainly preferable because they involve an atomic-scale mixing. An elevated level of interspersion can be maintained in the steps which follow up to the final product.

A method, based on a modified citrate route [11], is described in this paper. Although the citrate method may in principle be used with any anion, in practice due to the great solubility of nitrates it is practically restricted to these salts. The use of nitrates as starting materials assures the homogeneity of the solutions but leads (in the decomposition step or even in the concentration step) to an uncontrolled combustion [12] when copper is present and it was strongly non-recommended in the presence of silver even if the silver is present as only a few per cent [13]. The technique proposed here starts from an aqueous solution of the cations obtained by mixing salts of Y, Ba, Cu and Ag with citric acid and ammonium hydroxide; this technique makes no use of nitrates. The starting solution is then dried under vacuum. The solid so prepared is decomposed in an oxygen–nitrogen atmosphere at about 360 °C, thus giving a precursor containing well-interspersed yttrium oxide, barium carbonate, copper oxide and metallic silver.

The precursors obtained by this method, as well as by all methods which start from organic compounds, contain residual carbon (around 3 wt %) most of which can be ascribed to the presence of barium

---

*Author to whom correspondence should be addressed.

0022–2461 © *1994 Chapman & Hall*

carbonate. This carbon is not completely eliminated during calcination, and its segregation at 1–2–3 grain boundaries seems to be very harmful to the superconducting properties [9]. In order to reduce the carbon content the precursor powder was heated in a NO- or NO_2-containing atmosphere.

2. Experimental procedure

2.1. Preparation of the oxide-carbonate precursor

The preparation method included three steps. Since the dissolution of yttrium, barium, copper and silver using citric acid and salts which are readily available (but not nitrates) is a rather problematic task, we will give some experimental details of the preparation. An example is given for the production of 222 g of $YBa_2Cu_3O_{7-\delta}$/Ag (10 wt. %).

2.1.1. *Preparation of the starting solution*

A ratio of (Y): 100.36 g of yttrium acetate, $Y(CH_3COO)_3 \cdot 3.8(H_2O)$ (99.9% purity, Aldrich), was poured into 600 ml of water and the mixture was heated to 90 °C. A colourless and transparent solution (A) was obtained. Then 47.3 g of citric acid, $C_6H_8O_7 \cdot H_2O$ (99.8% Carlo Erba), was separately dissolved in 600 ml of water. This solution was added to the ice-cooled solution A, and a milky emulsion (B) was obtained. Next, 93 ml of ammonium hydroxide (30% Carlo Erba) was cooled in an ice bath and emulsion B was added to it. A colourless and transparent solution was obtained.

A ratio of (Ba): 101.60 g of barium peroxide BaO_2 (95% Fluka) was added, under strong stirring and at room temperature, to a solution obtained by dissolving 288.7 g of citric acid in 1000 ml of water. Then 271 ml of ammonium hydroxide was cooled in an ice bath and the barium solution was added to it. A colourless solution was added to it. A colourless solution was obtained; it was opalescent because of a slight gas bubble development which is believed to be oxygen released by BaO_2 decomposition and therefore a sign of barium complexation.

A ratio of (Cu): 179.69 g of copper acetate $Cu(CH_3COO)_2 \cdot H_2O$ (99% Carlo Erba) was dissolved in 300 ml of water at room temperature together with 94.3 g of citric acid. The solution was ice cooled after dissolution and 170 ml of ammonium hydroxide was added to give a transparent solution of intense blue colour.

A ratio of (Ag): 34.96 g of silver nitrate $AgNO_3$ (63.5% silver content, Johnson Matthey) was dissolved in 120 ml of water. Then 210 ml of tetramethylammonium hydroxide (10% Merck) was added. The Ag_2O precipitate so formed was washed on a filter until a neutral pH was recorded for the filtered water. Then 15.9 g of citric acid was dissolved in 600 ml of water and Ag_2O was added. The resulting suspension was ice cooled and 240 ml of previously cooled ammonium hydroxide were added. A clear solution containing silver was obtained.

In an ice bath, the yttrium-containing solution and then, with caution, the barium-containing solution were added to the solution containing copper. This solution was partially evaporated under vacuum in a rotary evaporator at 80 °C; then the silver-containing solution was added.

2.1.2. *Drying of the solution*

The solution was then placed into a rotary evaporator at 80 °C and dried under vacuum until a homogeneous viscous product was obtained. During this operation the colour turned from dark blue to dark green. Then the viscous slurry so obtained was dried in a vacuum oven. After a treatment at 90 °C for about 48 h a coarse grinding was carried out. The product was then heated first to 110 °C for 24 h and then to 170 °C for 24 h.

2.1.3. *Decomposition of the organic matter*

The product of the second step, a black powder, was ground to a particle size of less than 297 μm (48 mesh) and it was then placed in a downwards-gas-flow reactor (Fig. 1). The use of a downwards-gas-flow reactor avoided powder drag and allowed a high gas-flow rate (around $8\,l\,m^{-1}$) in order to reduce the duration of the decomposition. The gas was initially nitrogen, for 15 h at 200 °C. After this initial

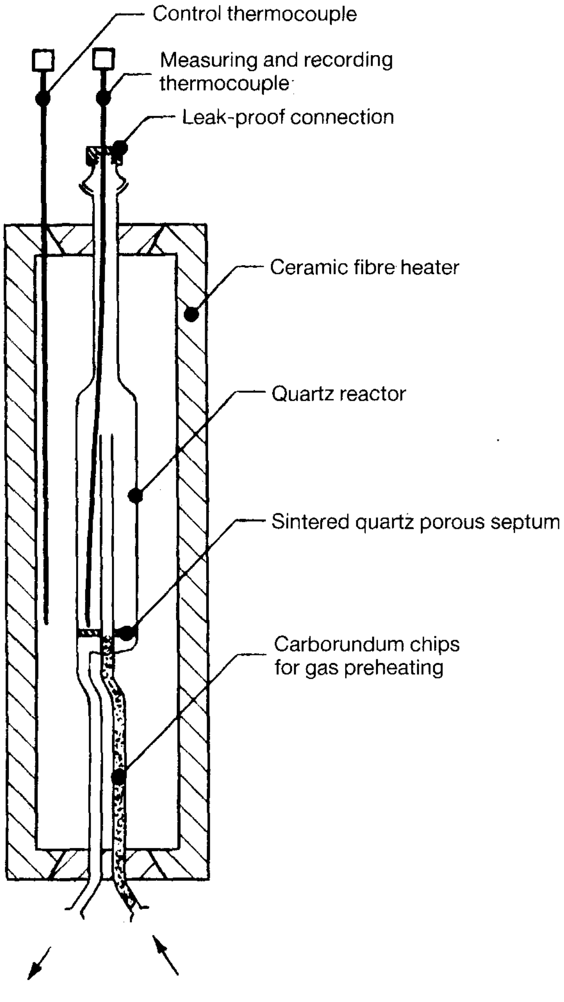

Figure 1 The gas-flow reactor.

conditioning period, a slow oxidative decomposition was started and controlled according to two criteria: (a) the temperature difference between the reactor's interior and the furnace, (the difference (due to the reaction heat) had to be less than 20 °C); (b) the oxygen consumption of the precursor (which had to be less than 1% of the total flow of oxygen and nitrogen). To fulfil these criteria, the oxygen percentage was kept at very low values (1%) for most of the overall heating time. Only at the end was the oxygen partial pressure gradually increased to 100% at temperatures around 400 °C. A typical decomposition scheme is shown in Fig. 2.

2.2. Processing of the powder in an atmosphere containing nitrogen oxides

Various samples of the precursor powder obtained were then heated in a NO- or NO_2-containing atmosphere. In a typical NO or NO_2 processing experiment, 40 g of the starting powder were placed inside a quartz gas-flow reactor. A mixture of NO (1.5%) in N_2 or of NO_2 (3%) in air was added to oxygen (80%) and then it was flowed over the sample. The temperature was ramped (150 °C h^{-1}) to the desired anneal temperature with a 20–90 h final holding. In most cases, following the NO annealing, the gas was switched to pure oxygen and the temperature was adjusted to the oxygen annealing temperature and held for 12–45 h and then cooled in the furnace to room temperature. In order to make sure that thermodynamic equilibrium between NO, NO_2, and O_2 could be more effectively reached, the oxygen was ozone enriched by allowing it to flow through an ozonizer consisting of four Berthelot tubes whose electrodes were charged at 15 kV.

2.3. Calcination–sintering

The NO-treated powder was then cold pressed into pellets 13 mm in diameter and 2 mm thick by applying a uniaxial pressure of 150 MPa. The pellets were calcined and sintered at different temperatures (890–950 °C) for 12 h in flowing oxygen and then they were slowly cooled at a rate of 30 °C h^{-1}.

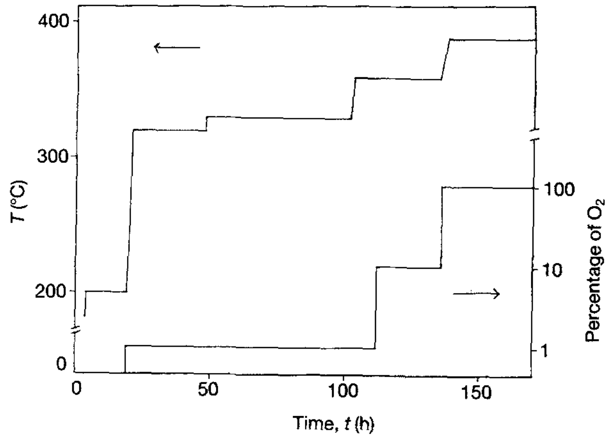

Figure 2 A decomposition scheme showing the temperature and oxygen profile versus the time on stream.

2.4. Materials characterization

Analysis of the carbon, nitrogen and hydrogen contents for the powders obtained at the various stages of the preparation process was carried out using an elemental analyser (EA 1108 Carlo Erba Instrumentations). The materials were also characterized by X-ray diffraction (XRD) (Philips PW1710, CuK_α), infrared (i.r.) spectroscopy (Perkin Elmer FTIR 1720 X), scanning electron microscopy (SEM) and energy dispersive analysis of X-rays (EDAX) (JEOL and Cambridge Instruments). The density of the sintered pellets was measured with a macropores unit (Carlo Erba) using mercury intrusion up to 100 kPa. Magnetic susceptibility measurements versus the applied field at 77 K were performed on sintered pellets using an alternating current (a.c.) susceptometer.

3. Results and discussion

3.1. Precursor characterization

Data on the powder weight observed in four different preparations are given in Fig. 3. The carbon, nitrogen and hydrogen contents (wt %) are shown in Fig. 4. In Figs. 3 and 4 $P_{YBCO-Ag}$ is the weight of the composite

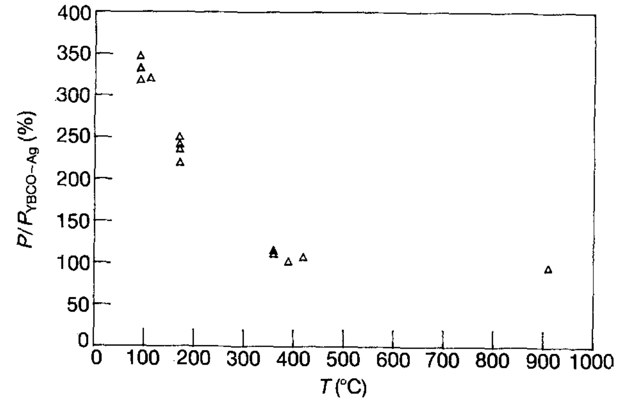

Figure 3 Powder weight versus the maximum temperature reached during thermal treatment. $P_{YBCO-Ag}$ is the weight of the composite ceramic (1–2–3/Ag) at the end of the preparation process. The points are reffered to four different preparations.

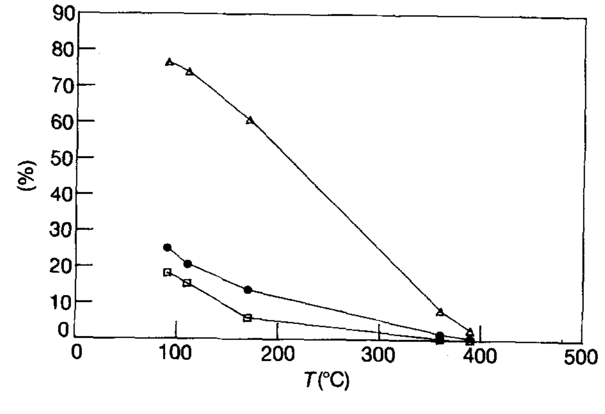

Figure 4 The carbon, nitrogen and hydrogen contents versus maximum temperature, *T*, reached during the exsiccation and decomposition thermal treatment; (△) $P_C/P_{YBCO-Ag}$, (●) $P_N/P_{YBCO-Ag}$, and (□) $P_H/P_{YBCO-Ag}$. The data are given as the weight of the element divided by $P_{YBCO-Ag}$ (the weight of the composite ceramic (1–2–3/Ag) at the end of the preparation process).

ceramic (1–2–3/Ag) at the end of the preparation process while T is the maximum temperature reached during the thermal treatment. It is evident that the weight loss, associated with the decomposition/oxidation of the organic fraction of the precursor is almost complete at around 400 °C. The small weight loss observed up to 910 °C may be attributed to $BaCO_3$ decomposition, as shown by XRD and i.r. analyses. After the final annealing in pure oxygen at around 400 °C, the carbon content of the precursor powder was analysed as 2.72%, which is lower than the value expected (2.93 wt %) if all the barium is combined as carbonate. The nitrogen and hydrogen contents were found to be 0.34% and 0.02%, respectively. The presence of nitrogen may be ascribed to the formation of a small quantity of barium nitrate.

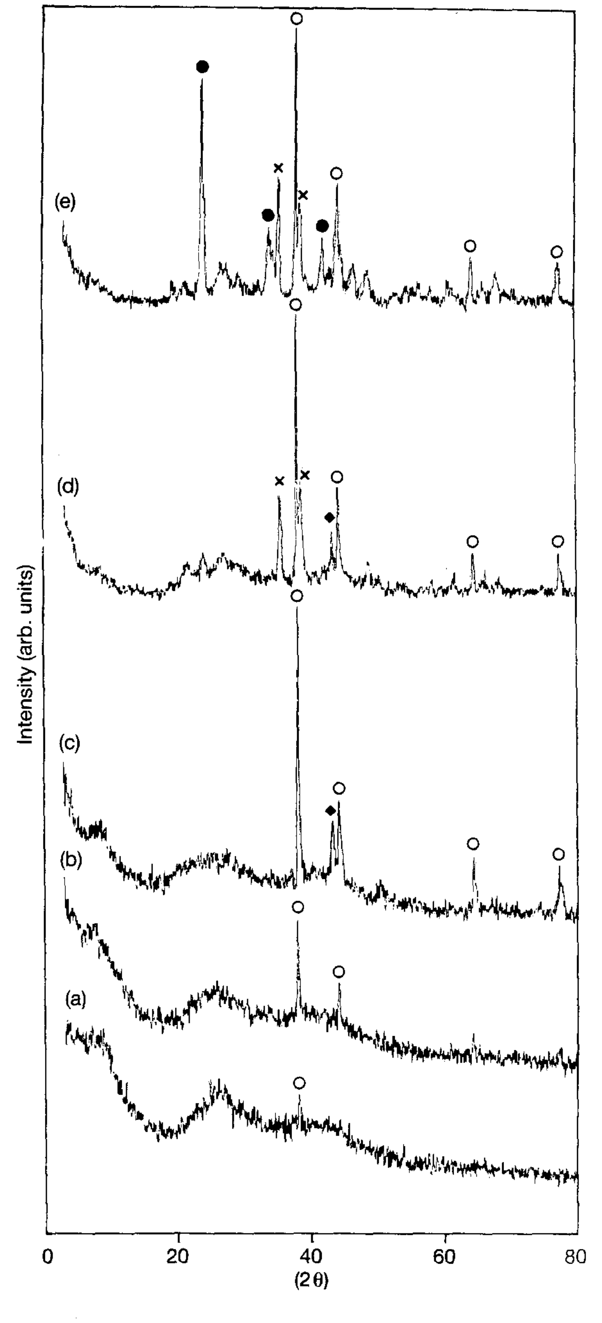

Figure 5 XRD spectra for various powders, showing the crystalline phase evolution during various stages of the exsiccation and decomposition process: (●) $BaCO_3$, (×) CuO, (○) Ag, and (◆) Cu; (a) 90 °C, (b) 110 °C, (c) 170 °C, (d) 360 °C, and (e) 390 °C.

The XRD spectra of the powders obtained at the various stages of the decomposition process are shown in Fig. 5. It is noteworthy that metallic silver forms from the amorphous gel during the exsiccation at 90–110 °C (Fig. 5a and b). After exsiccation at 170 °C (Fig. 5c) copper also separates as a metal without forming an Ag–Cu alloy. It is also noteworthy that during the decomposition of the organic matter carried out in an O_2-containing atmosphere copper only transforms to copper oxide, while silver remains in the metallic form (Fig. 5d, e). At the end of the oxidative decomposition, the precursor powder has an XRD spectrum in which copper oxide, barium carbonate and metallic silver are easily detected (Fig. 5e). No phase ascribable to the presence of yttrium in the powder was found in the XRD spectra, probably because yttrium oxide is present as an amorphous or microcrystalline phase.

To show the level of interspersion of the metal ions, a precursor powder was examined using a scanning electron microscope equipped with an energy dispersive analyser of X-rays. Yttrium, barium, copper and silver appear to be well-interspersed, as shown by the corresponding elemental maps (Fig. 6).

3.2. Characterization of nitrogen oxide processed samples

To reduce the carbon content a sample of the precursor powder was annealed in a NO-containing atmosphere at 280 °C for 20, 40 and 90 h. Carbon- and nitrogen-content measurements were performed by elemental analysis while a quantitative evaluation of the presence of $BaCO_3$ and $Ba(NO_3)_2$ was carried out by XRD and i.r. analysis. Fig. 7a gives the residual carbon content shown by elemental analysis, by the intensity of the 695 cm^{-1} i.r. peak (typical of $BaCO_3$) and by the 0.369 nm line in the XRD spectra, taking the respective intensities and the carbon content of the precursor as references (1 0 0). Fig. 7b gives the nitrogen content shown by elemental analysis, by the intensity of the 730 cm^{-1} i.r. peak (typical of $Ba(NO_3)_2$) and by the 0.468 nm line in the XRD spectra, taking the respective intensities and the nitrogen content of the 90 h nitrogen-oxide-processed sample as references (1 0 0). It can be concluded that NO processing reduces the carbon content in the precursor powder by converting $BaCO_3$ to $Ba(NO_3)_2$ as shown by XRD patterns (Fig. 8). However this conversion is not complete: a fraction of $BaCO_3$ is readily converted to $Ba(NO_3)_2$ after a 20 h anneal; subsequent anneals are not substantially able to further reduce the carbon content. After 90 h, the carbon content was analysed to be 0.60%, which is equivalent to 27.5% of the starting value.

Very similar results were obtained using NO_2 instead of NO. Since NO_2 is a vapour which is much more complicated to manipulate than NO, more attention was given to NO.

To investigate the effect of the NO annealing temperature on the carbon content, five samples of the same starting precursor powder were heated in a NO-

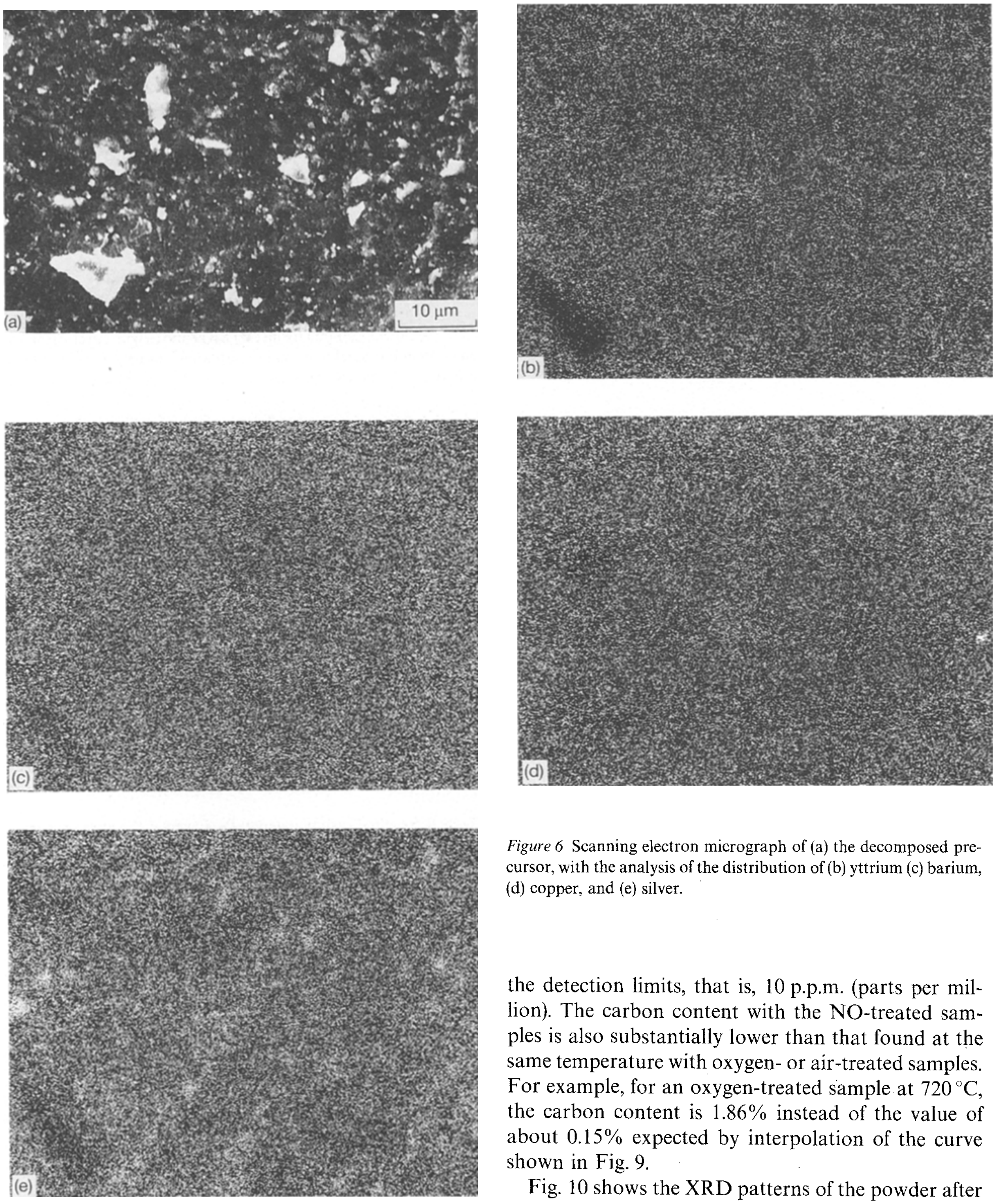

Figure 6 Scanning electron micrograph of (a) the decomposed precursor, with the analysis of the distribution of (b) yttrium (c) barium, (d) copper, and (e) silver.

containing atmosphere at 460, 560, 760, 860, 950 °C for 22 h. The samples heated at 460 and 560 °C were further annealed in oxygen at 560 °C for 45 h to decompose the $Ba(NO_3)_2$ which eventually formed. The samples heated at 760, 860 and 950 °C were then oxygen annealed for 12 h at the same NO annealing temperature. Carbon-content measurements were performed on the NO processed samples and the results are shown in Fig. 9. These data indicate that raising the NO annealing temperature reduces the carbon content of precursor powder. After annealing at 950 °C the carbon content was analysed to be under the detection limits, that is, 10 p.p.m. (parts per million). The carbon content with the NO-treated samples is also substantially lower than that found at the same temperature with oxygen- or air-treated samples. For example, for an oxygen-treated sample at 720 °C, the carbon content is 1.86% instead of the value of about 0.15% expected by interpolation of the curve shown in Fig. 9.

Fig. 10 shows the XRD patterns of the powder after the NO treatment and the oxygen annealing. The XRD spectrum for the 460 °C NO-treated powder was not distinguishable from the 560 °C annealed powder and is therefore not included. In the 560 °C annealed-powder spectrum (Fig. 10a) the absence of characteristic peaks of $BaCO_3$ and $Ba(NO_3)_2$ was evident, the only phase containing barium being $Ba_2Cu_3O_{5.9}$ (probably because the BaO formed reacts with CuO). This phase is present in the CuO–BaO–$YO_{1.5}$ pseudo-ternary system, but it is not usually formed as an intermediate compound in 1–2–3 synthesis; its formation seems to be a peculiarity of this method of preparation. The YBCO phase had already formed at a temperature of about 760 °C (Fig. 10b). At temperatures higher than 760 °C, traces of the 2–1–1 phase were detected (Fig. 10b to d).

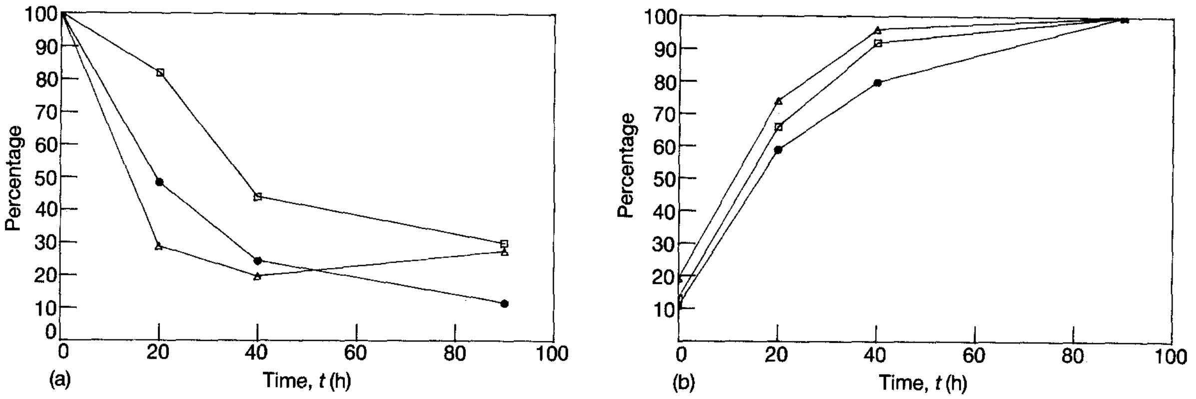

Figure 7 (a) (△) Carbon-content measurements and quantitative evaluation of the $BaCO_3$ content (from (●) XRD and (□) i.r. spectra) for the same powder after different NO annealing times at 280 °C. (b) (△) Nitrogen-content measurements and quantitative evaluation of $Ba(NO_3)_2$ content (from (●) XRD and (□) i.r. spectra) for the same powder after different NO annealing times at 280 °C. For more details see text.

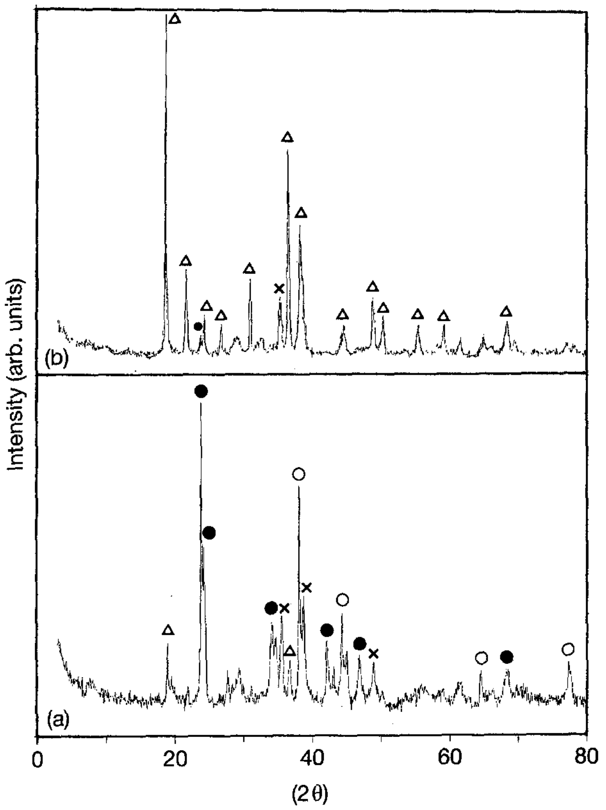

Figure 8 XRD spectra for an (a) 0 h and (b) 90 h NO annealed powder at 280 °C showing the partial conversion of $BaCO_3$ to $Ba(NO_3)_2$: (●) $BaCO_3$, (△) $Ba(NO_3)_2$, (×) CuO, and (○) Ag. The total gas flow used was 2.5 l min^{-1}.

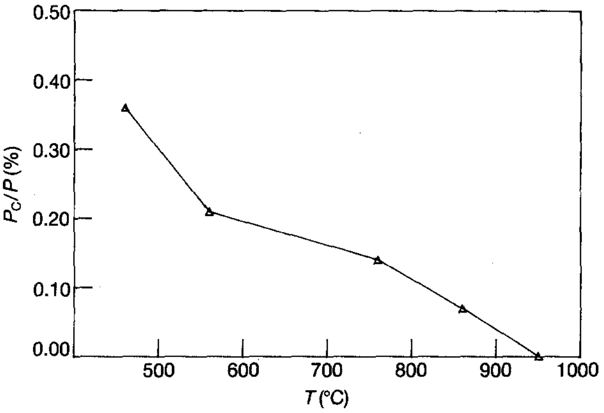

Figure 9 Residual carbon content, P_C/P, versus the annealing temperature of NO-treated powders.

3.3. Characterization of sintered pellets

Various samples of NO-treated powders were then pelletized and sintered at different temperatures in the range 890–950 °C. XRD results for ground samples from the pellets (Fig. 11) show that the traces of the 2–1–1 phase completely disappeared with the formation of the pellet and the subsequent final anneal; the XRD patterns show the presence of only two phases: silver and orthorhombic 1–2–3. In contrast, the formation of a 2–1–1 phase and also of $BaCuO_2$ was evident (Fig. 12) in a sintered pellet obtained from a sample of the precursor powder which was not oxygen annealed after the NO treatment at 460 °C. Thus it seems that the presence of some nitrate can promote the formation of spurious phases in sintered pellets.

Carbon-content measurements were also performed, but the results showed that the carbon content was under the detection limit (10 p.p.m.) of the elemental analyser.

Table I gives the results of the pellet density measured on the samples NO-treated at 560, 760, 860, 950 °C, formed in a pellet and finally sintered at 950 °C. The density is given as a percentage of the structural density, assuming the density of YBCO to be 0.638 kg m^{-3}, that of silver to be 1.053 kg m^{-3} and the volumes to be additive. It appears that density is rather low in its absolute value, slowly decreasing with the NO treatment temperature in the 560–860 °C range and having a more substantial drop for the sample treated at 950 °C. This drop is probably related to the fact that at 950 °C silver is liquid in an oxygen atmosphere.

SEM/EDAX analysis (Fig. 13) was performed for three 910 °C sintered pellets obtained from three samples of powder NO-treated at different temperatures (560, 760, 860 °C). The scanning electron micrographs of the pellet surface and the corresponding elemental map shows that the silver distribution depends on the

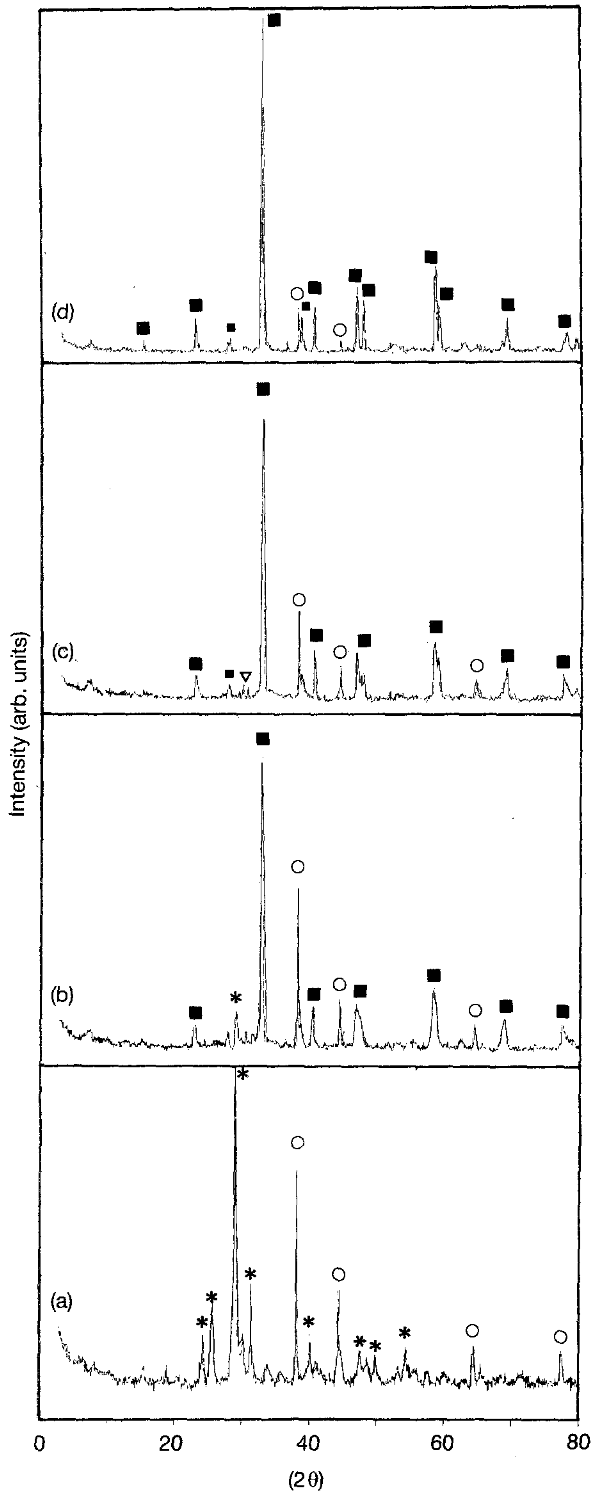

Figure 10 XRD spectra for four powders (■) $YBa_2Cu_3O_{7-\delta}$, (▽) Y_2BaCuO_5, (∗) $Ba_2Cu_3O_{5.9}$ and (○) Ag. NO-treated and oxyger annealed at four different temperatures: (a) 560 °C, (b) 760 °C, (c 860 °C, and (d) 950 °C.

TABLE I The pellet densities of samples sintered at 950 °C obtained from powders treated with NO at different temperatures

NO anneal temperature (°C)	Pellet density (kg m^{-3})	Percentage of the theoretical density
560	5.440	81.9
760	5.370	80.1
860	5.270	79.4
950	4.770	71.8

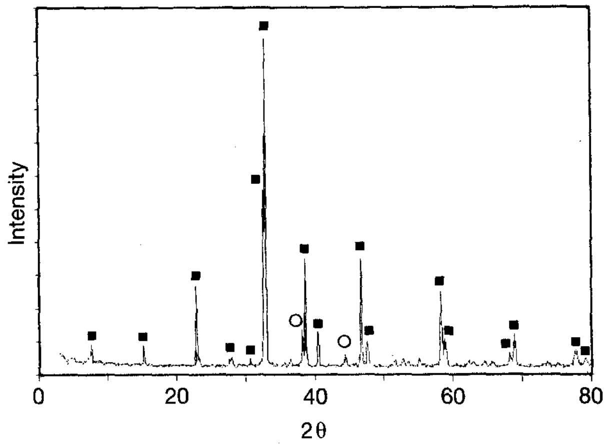

Figure 11 An XRD spectrum of a sample ground from a 950 °C sintered pellet: (■) $YBa_2Cu_3O_{7-\delta}$, and (○) Ag.

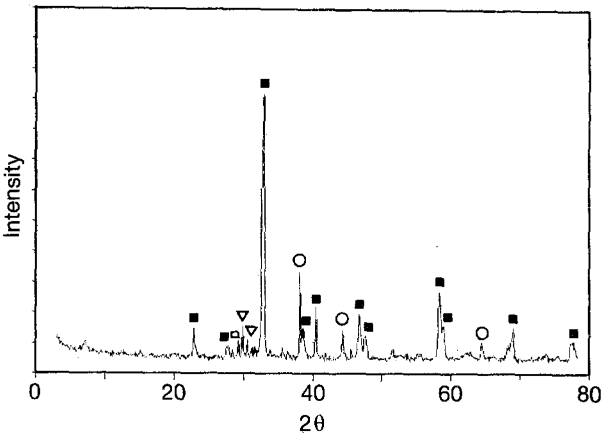

Figure 12 An XRD spectrum of a sample ground from a sintered pellet obtained from the precursor powder which was not oxygen annealed after the NO treatment: (■) $YBa_2Cu_3O_{7-\delta}$, (▽) Y_2BaCuO_5, (□) $BaCuO_2$, and (○) Ag.

NO annealing temperature. A more uniform distribution was obtained starting from higher-temperature NO-treated precursor powders.

Magnetic susceptibility measurements at 77 K were performed over sintered pellets. Fig. 14 shows the results for four 950 °C sintered pellets obtained from precursor powders which were NO-treated at different temperatures (560, 760, 860, 950 °C) and oxygen annealed as previously described (and therefore they had different carbon contents: 0.21, 0.14, 0.07, and less than 0.001 wt %. The best current transport properties are shown by a sample whose precursor powder has a very low (0.07%), but not the lowest, value for its carbon content. The lower susceptibility values measured for the sample NO-treated at 950 °C may be attributed to the lower pellet density, but at this stage we cannot exclude (for this temperature of NO-treatment) the possibility that important amounts of silver enter the YBCO structure thus lowering the superconducting properties. Therefore it seems that improved magnetic properties depend on a low carbon content in the precursor powder, although this is not the only critical parameter.

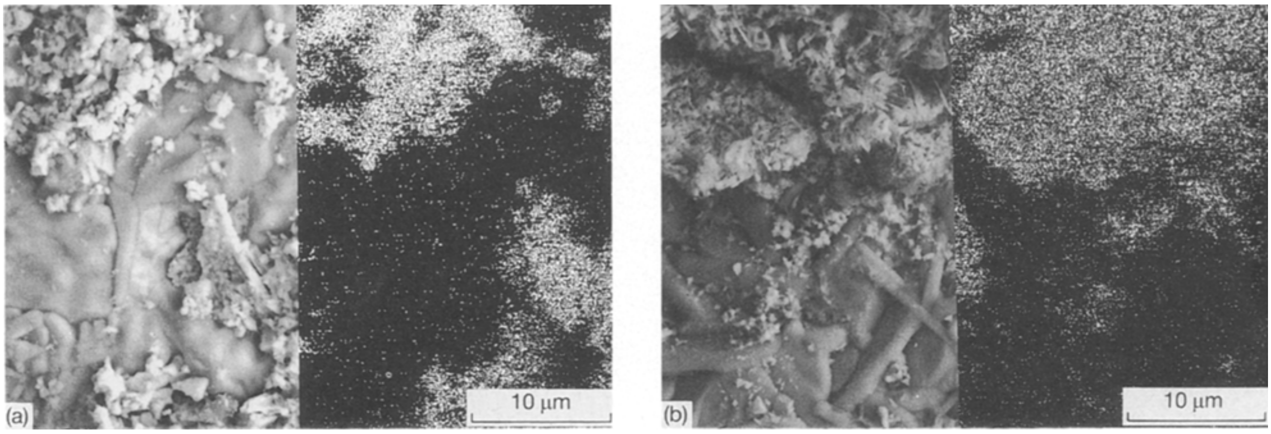

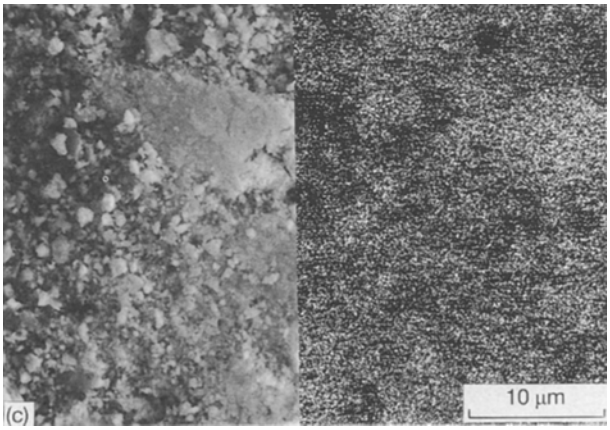

Figure 13 Scanning electron micrographs and silver elemental maps for the surface of three 910 °C sintered pellets obtained starting from precursor powders which were NO-treated at temperatures of: (a) 560 °C, (b) 760 °C, and (c) 860 °C.

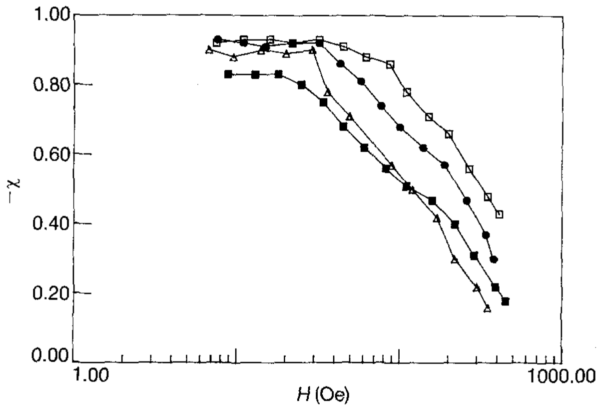

Figure 14 Magnetic susceptibility versus applied-field measurements for four 950 °C sintered pellets obtained from powders which were NO treated at (△) 560, (●) 760, (□) 860 and (■) 950 °C.

4. Conclusions

In this work some details were given of a wet preparation of composite $YBa_2Cu_3O_{7-\delta}/Ag$ ceramics in which silver is introduced directly in form of a solution. The preparation is a modification of the citrate method which does not utilize nitrates as starting salts, thus allowing for a smooth and controlled decomposition of the organic substance.

We also described a method for lowering the carbon content, using a nitrogen-monoxide enriched atmosphere (0.3% NO in a O_2–N_2 mixture). This treatment also distributes silver more uniformly in the powder, probably by spreading it on the surface of the grains.

Although the magnetic-susceptibility characteristics are not exceptional, these can probably be ascribed to the low density of the materials (70–80% of the theoretical value). Further work to increase the density of the sintered materials, for example, using the powder in a tube technique, is expected to improve the superconducting characteristics substantially.

Acknowledgements

We thank: the CNR and the INFM for financial support; A. Santucci and M. Bodini (Snamprogetti) for the carbon, nitrogen and hydrogen-content determinations; G. Gasti for the pellet-density measurements; and L. Gherardi and P. Caracino (Pirelli Cavi S.p.A.) for the magnetic susceptibility measurements.

References

1. B. R. WEINBERGER, L. LYNDS, D. M. POTREPKA, D. B. SNOW, C. T. BURILA, H. E. EATON JR., R. CIPOLLI, Z. TAN and J. I. BUDNICK, *Physica C* **161** (1989) 91.
2. L. GANAPATHI, A. KUMAR and J. NARAYAN, *J. Appl. Phys.* **66** (1989) 5935.
3. A. GOYAL, S. J. BURNS and P. D. FUNKENBUSCH, *Physica C* **168** (1990) 405.
4. J. P. SINGH, H. J. LEU, R. B. POEPPEL, E. VAN VOORHEES, G. T. GOUDEY, K. WINSLEY and D. SHI, *J. Appl. Phys* **66** (1989) 3154.
5. T. NISHIO, Y. ITOH, F. OGASAWARA, M. SUGANUMA, Y. YAMADA and U. MIZUTANA, *J. Mater. Sci.* **24** (1989) 3228.
6. B. DWIR, M. AFFRONTE and D. PAVUNA, *Appl. Phys. Lett.* **55** (1989) 399.
7. Y. H. KAO, Y. D. YAO, L. Y. JANG, F. XU, A. KROL, L. W. SONG, C. J. SHER, A. DAROVSKY, J. C. PHILLIPS, J. J. SIMMINS and R. L. SNYDER, *J. Appl. Phys.* **67** (1990) 353.
8. Y. MATSUMOTO, J. HOMBO and Y. YAMAGUCHI, *Mater. Res. Bull.* **24** (1989) 1231.
9. D. R. CLARKE, T. M. SHAW and D. DIMOS, *J. Amer. Ceram. Soc.* **72** (1989) 1103.
10. T. L. WARD, T. T. KODAS, A. H. CARIM, D. M. KROEGER and H. HSU, *J. Mater. Res.* **7** (1992) 827.
11. P. L. VILLA, PCT patent application PCT/EP91/02404 filed on December 13 1991.
12. F. CELANI, R. MESSI, S. PACE and N. SPARVIERI, *Il Nuovo Saggiatore* **4** (1988) 7.
13. P. COURTY, H. AJOT, C. MARCILLY and B. DELMON, *Powder Technol.* **7** (1973) 21.

Received 9 September 1993
and accepted 6 January 1994